2018 EAGE ANNUAL
80TH CONFERENCE + EXHIBITION
COPENHAGEN | DENMARK

Automated salt-model building using constrained FWI

Guasch L [2] , Lin T [2] , Herrmann F [3] , Warner M [1]
[1] Imperial College, London, UK
[2] S-Cube, London, UK
[3] UBC, Vancouver, Canada, now at: Georgia Tech, Atlanta, USA

Introduction

Building accurate velocity models over large complex salt bodies is typically slow, expensive and non-unique, but is essential for accurate depth imaging of salt-affected surface seismic data. Typical workflows involve many passes of reflection tomography, depth migration followed by picking of top salt, salt flooding, re-migration, picking base salt, sediment flooding, re-migration, manual identification of salt inclusions, carapaces, dirty salt and other anomalies, and repeated scenario testing through re-migration to refine model details. Full-waveform inversion is often integrated into this workflow, but typically it is used only to tweak shallow fine detail rather than to build significant portions of the velocity model at greater depths.

Here we present an alternative approach, and demonstrate its application to a complicated 3D synthetic salt body that contains all of the structural elements that typically make salt-model building difficult. We begin from a starting model that is smooth and simple; such a model is straightforward to obtain from pre-stack migrated gathers without picking salt boundaries. We obtain the velocity model, using raw field data containing multiples, ghosts, reflections and refractions, by applying a form of FWI that is robust against cycle skipping coupled with the automatic application and successive relaxation of constraints on the recovered model. Using this approach, with realistic frequencies and acquisition geometries, we are able to recover the salt body accurately to depths of about 5000 m, including rugose top salt, salt welds and inclusions, carapaces, salt flanks and over-hangs, and successfully recover migrated interfaces below base salt to depths of around 8 to 10 km.

Method and model

We invert salt-affected data using a version of FWI that has the following characteristics:

- It uses the adaptive waveform inversion (AWI) objective function of Warner & Guasch (2016) rather than the least-squares-difference objective function typical of conventional FWI. The use of AWI provides robustness against cycle skipping and enables the use of a low-accuracy start model.
- It applies several constraints to the model that are progressively relaxed as the inversion proceeds. These include constraints on the total variation of the model, and asymmetric hinge-loss total variation (ATV) applied in a vertical direction as described by Esser et al. (2016; 2018). The latter acts implicitly to flood velocities downwards from any boundary, initially flooding salt or carapace velocities to the base of the section, and later flooding sediment velocities beneath base salt. Note that this flooding is entirely implicit, it does require explicit identification of salt boundaries.
- It uses only a small random subset of sources at each iteration. Iteration proceeds from low to high frequencies by opening up the pass band while the constraints are gradually relaxed. Once the highest frequency is reached, the sequence is repeated as a warm start, and the constraints are further relaxed. Initially, the constraints serve to guide the model away from implausible models, and as the constraints are relaxed, the data come to dominate the inversion.
- It pays most attention to the kinematics of the data, damping amplitude effects that it cannot easily match while still having regard for those amplitude characteristics that may contain useful useable information when inverting elastic attenuative variable-density data. This characteristic is not especially important when inverting synthetics, but it is essential for the inversion of field data.

The model we use to demonstrate the method is shown in Figures 1a, 2a and 3a, taken from the SEAM sub-salt GoM dataset, at full scale and full depth. The model measures 21 × 18 km laterally, and is 15 km deep. It contains a complicated salt body, with a rugose top, an overlying carapace of slightly reduced velocity which conventional workflows will typically misidentify as faster salt, geometrically complicated overhangs and flanks, and internal low-velocity inclusions and salt welds. We generated isotropic acoustic synthetic data over this model using a realistic density model, a free surface, and 1050 sources and 150,000 receivers located at 15 m depth. The data are full-azimuth with a maximum offset of 27 km in the centre of the model decaying to narrow azimuth and reduced offset towards the sides and corners of the model. The water depth is variable around 1200 m.

Results

Shen et al. (2017) reported that the lowest frequencies useable for FWI on the Gulf of Mexico Atlantis node dataset were below 2 Hz. Consequently we here begin the inversion from 2 Hz, extending the pass band eventually to 7 Hz in ten stages. We used 10% of the sources at each iteration, touching each source once before moving to the next pass band, giving ten iterations per source in total. The total-variation and ATV constraints were reduced at each iteration, accelerating as the inversion proceeded. Two passes were used in total, the second beginning again from 2 Hz, giving 40 iterations per source for the final model. Although the data were generated using a realistic density model, the inversion did not have access to that model so that this is not an inverse-crime inversion.

The starting model for the inversion is shown in Figures 1b and 2b. The start model is smooth; it does not contain any of the details of the geometry of the salt body, it does not contain the correct salt velocity, and it does not contain the correct post-salt or intra salt sedimentary velocities. It does contain the correct water velocity and the correct geometry of the seabed, and importantly it does contain a generic high-velocity body in the approximate location of the true salt body. Our inversion can be made to work without any indication of high salt velocities, but in these circumstances it takes very many iterations to reach the true model, and it will always be less computationally expensive to begin closer to the true model. Crucially, the start model does not represent a smoothed version of the true model so that the inversion must be capable of both overcoming cycle skipping and of shifting the long-wavelength bulk velocity of the model – compare for example Figures 1a and 1b.

We first tested conventional FWI on this problem, Figure 2c, without using model constraints or an algorithm with robustness to cycle skipping. We also tested conventional FWI with constraints but without AWI, and we tested AWI without constraints. None of these flavours of FWI were able to recover the true model adequately. Without constraints, both FWI and AWI perform a reasonable job, migrating top salt into the starting model, improving supra-salt and intra-salt sedimentary velocity structure, and recovering some portions of the deeper salt boundaries. Without constraints though, these algorithms are not able to recover accurate velocities within the salt, and are unable to flood a coherent salt body unless this body already exists substantially within the starting model – see Figure 2c for the FWI result. Without AWI, but with constraints, parts of the data are unable to recover from cycle skipping, leading to spurious ragged artefacts appearing adjacent to salt boundaries; typically these display salt-like velocities outside the salt and sediment-like velocities inside.

Figures 1c, 2d and 3b show the final model recovered when using both AWI and ATV together. This combination is sufficient both to overcome the inadequacies of the start model and to flood the salt and sub-salt model accurately. Figures 2d and 3b show that the salt boundary is recovered to a depth of at least 5000 m, below which the quality slowly decreases. Away from the survey edges, the rugose top of salt, bottom salt, salt flanks and salt overhangs are all accurately recovered. Top salt in particular is recovered to an accuracy in depth that closely matches the half-wavelength achievable at 7 Hz. The inversion is also able to capture accurately the overlying slightly lower velocity carapace, together with salt welds and inclusions within the salt, where again the resolution is limited only by the seismic wavelengths used in the inversion. Recovery of the carapace is seen especially clearly in the 3000-m depth slice in Figure 3. Conventional workflows have difficulty in identifying fast layers that immediately overlie salt, and these will often consequently be assigned salt velocity. In this inversion, the velocity and geometry of the carapace is recovered automatically.

In most places, sedimentary velocities are well recovered down to about 5000 m, as can be seen clearly in Figure 3. In some places however, there is minimal data available to constrain sedimentary velocities accurately, especially towards the edges of the survey area where there is limited azimuthal coverage. This effect is visible on the right side of the lower panel in Figure 1c – here, even though the constraints have been weakened considerably, the sedimentary velocity model is still dominated by the constraints and not the data. Below the salt, and below depths of about 5 km, the absolute velocities are not well recovered, but the boundaries between sedimentary layers are properly recovered to about 10 km depth indicating that the model will correctly migrate sub-salt reflectors.

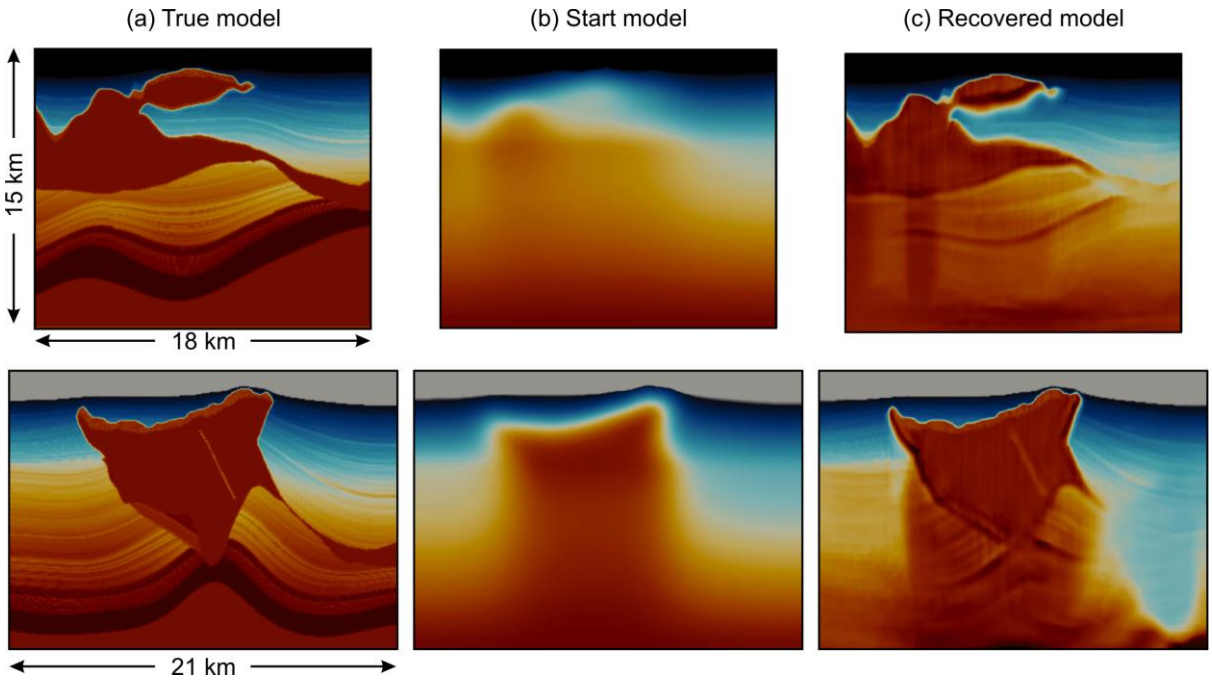

Figure 1 *In-line and cross-line vertical sections through the (a) true, (b) starting, and (c) final recovered velocity models. The 3D model measures 21 × 18 × 15 km.*

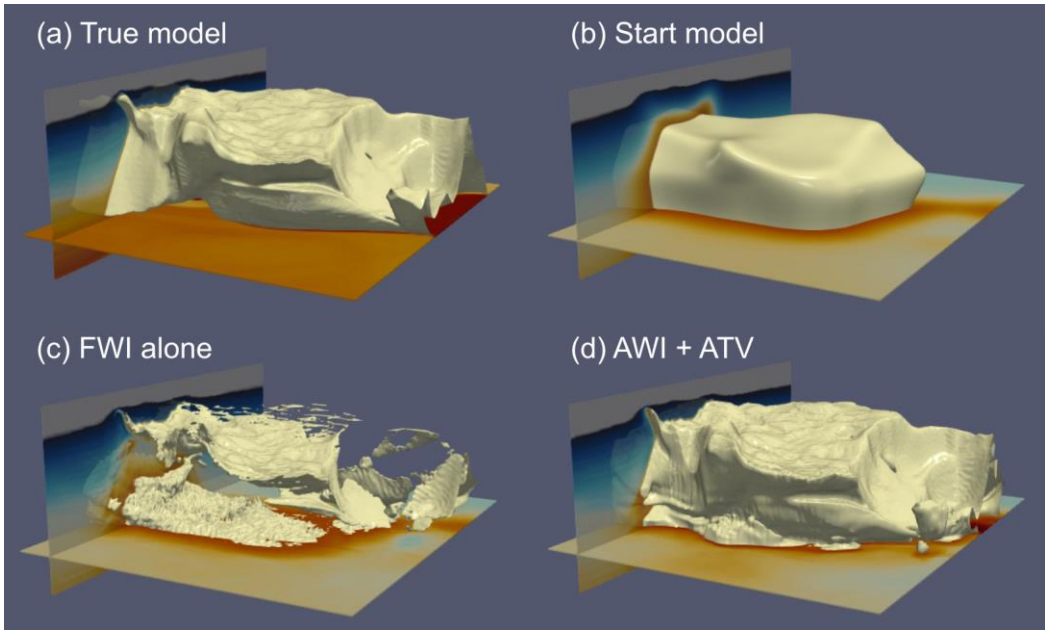

Figure 2 *Iso-velocity surface, at 4000 m/s, showing the location of the salt body in the (a) true, (b) starting, (c) conventional FWI-recovered, (d) AWI-plus-ATV-recovered models. The horizontal plane is at a depth of 7300 m; colours on the vertical plane show velocity.*

We also tested inversions with and without a free surface; including multiples in the inversion is not normally detrimental and can help to improve the final model. We also tested inversion with and without an accurate density model in the inversion; the latter is always helpful but is not essential. We have not yet tested the scheme using full-elastic or attenuating synthetic data. Tests in 2D suggest that a simple matching scheme (Calderon Agudo et al., 2017) will provide sufficient robustness against the AVO and phase changes introduced by attenuation and elasticity.

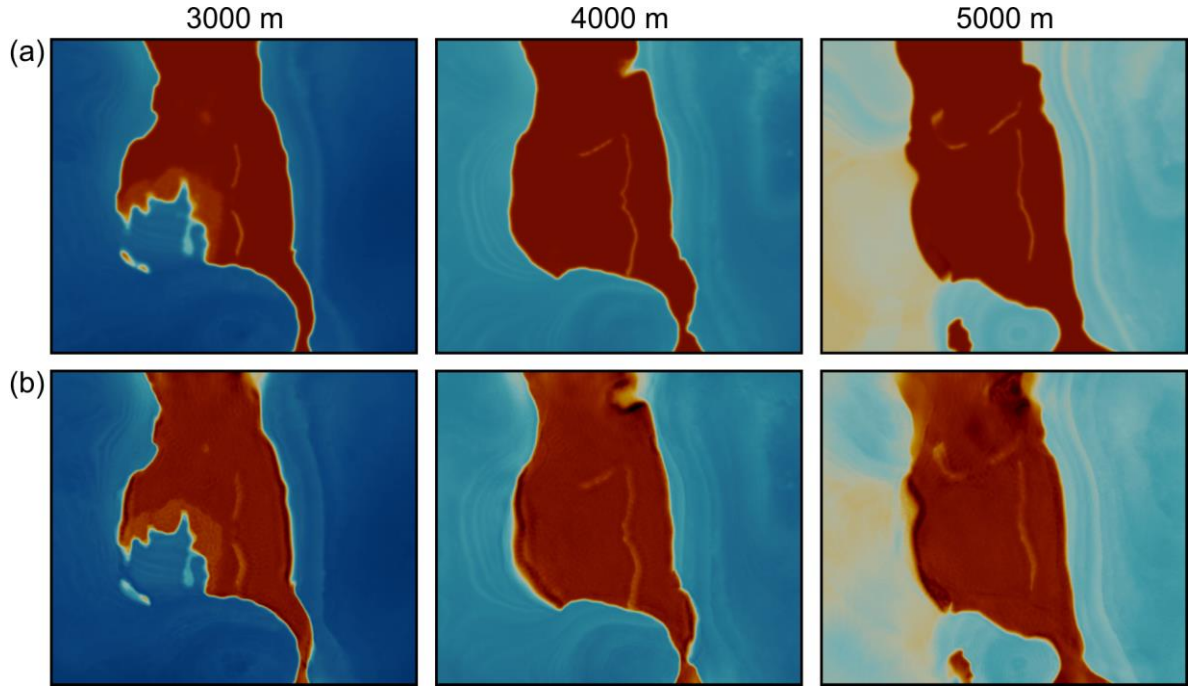

Figure 3 *Horizontal depth slices through the salt body, at 3, 4 and 5 km depth, for the (a) true, and (b) final recovered models. Away from survey edges, the salt geometry, salt inclusions, velocity in the carapace (seen at 3000 m depth, centre left of the salt), and sediment velocities are all well recovered.*

Conclusions

Unlike conventional workflows, FWI that is suitably constrained and robust against cycle skipping, can recover an accurate salt model from raw seismic data without recourse to intensive time-consuming repeat migration, explicit picking of salt boundaries, or detailed scenario testing. The combination of adaptive waveform inversion with total-variation and asymmetric hinge-loss total-variation constraints on the model can realistically recover a high quality salt model to about 5000 m depth, and successfully migrate sub-salt sedimentary interfaces to about 10,000 m depth. The total elapsed time required by this approach is much shorter than that of conventional velocity model building for salt. It provides the promise of building the velocity model at least as rapidly as the reflection data can be processed, so that final depth migration happens much more rapidly. The machine time required for FWI is significant, but it will normally be less than that required for the repeated applications of reverse-time migration typically required by conventional workflows.

We thank S-Cube and SEAM for permission to publish. AWI & ATV are patented technologies.

References

Calderon Agudo et al. [2017] Addressing viscous effects in acoustic full-waveform inversion. 79th EAGE Conference and Exhibition, Extended Abstracts.

Esser et al. [2016] Constrained waveform inversion for automatic salt flooding. *The Leading Edge*, 35 (3), 235-239.

Esser et al. [2018] Total-variation regularization strategies in full-waveform inversion. SIAM Imaging Sciences, *in press*.

Shen et al. [2017] Salt model building at Atlantis with full-waveform inversion. 87th Annual International Meeting, SEG, Expanded Abstracts.

Warner & Guasch [2016] Adaptive waveform inversion: Theory. *Geophysics*, 81(6), R429-R445.